

# Gas Phase Epoxidation of Propene by Nitrous Oxide over Silica-Supported Iron Oxide Catalysts

Viorel Duma and Dieter Hönicke

*Department of Chemical Technology, Technical University of Chemnitz, 09107 Chemnitz, Germany*

Received August 11, 1999; revised November 23, 1999; accepted November 23, 1999

Catalysts consisting of sodium-promoted silica gel-supported iron oxide were found to catalyze the gas phase epoxidation of propene by nitrous oxide. Selectivities to propene oxide of 40–60% at propene conversions in the range of 6–12% were observed. The influence of different parameters on the yield to propene oxide is discussed: the amount and the dispersity of iron oxide, the procedure of alkali promotion, the morphology of the support, and the reaction parameters. © 2000 Academic Press

**Key Words:** propene oxide; epoxidation; gas phase; nitrous oxide; iron oxide catalysts.

## INTRODUCTION

Propene oxide is one of the most important organic intermediates and is used for the production of many useful chemicals. Today propene oxide is mainly manufactured by one of two commercial processes viz. the organic-hydroperoxide process or the chlorohydrin process (1a, 2), both of them performed in the liquid phase. The compulsory formation of a side product in the former and the chlorine used in the latter process are substantial drawbacks of these industrial processes. Therefore, the development of a process for the direct gas phase epoxidation of propene which overcomes these disadvantages would be of great economical importance.

Some alkenes like ethene and styrene, which have no allylic hydrogen atoms, can be directly epoxidized with molecular oxygen in the gas phase over Ag catalysts. The process for the direct epoxidation of ethene over Ag catalysts was developed in the past (1b) and has been performed worldwide for six decades. However, over the same or similar catalysts the propene oxidation leads to propene oxide selectivities of less than 15% at a conversion degree of less than 15% (2). Some recent patents claim that reaching high selectivities to propene oxide over novel supported precious metal catalysts is possible; however, the yields are generally under 1% (3, 4).

The interaction between molecular oxygen and metals or metal oxides will produce electrophilic and nucleophilic oxygen species. For the transformation of the vinyl group of an alkene in an oxirane ring, a mild electrophilic

oxygen species will be necessary. However, the molecular oxygen produces strong electrophilic oxygen species over noble metals and nucleophilic species over transition metal oxides.

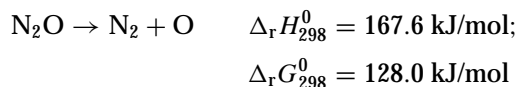
Generally, the reaction between oxygen species and a propene molecule will occur, dependent on the electronic properties of the oxygen species, following one of three possible reaction paths (Fig. 1):

1. The reaction between mild electrophilic oxygen species and propene will take place at the  $\pi$ -bond of propene. In this way will emerge propene oxide, propanal, and acetone. High temperatures and acidic or basic conditions will favor, directly or by the isomerization of propene oxide, the formation of propanal and acetone (1a, 2, 5), so that such circumstances have to be avoided in order to improve the selectivity to propene oxide.
2. Strong electrophilic oxygen species will attack all C–C bonds. Thus, the reaction products will be carbon oxides and organic molecules having one or two carbon atoms.
3. Nucleophilic oxygen species will attack preferentially H atoms in the allylic position. This reaction path will lead to products like allyl alcohol, acrolein, and acrylic acid.

A particular case is silver, which generates a mild electrophilic, peroxide-like oxygen species but a nucleophilic one as well. Therefore, alkenes which have no allylic hydrogen atoms can be selectively oxidized to epoxides over Ag catalysts. However, alkenes such as propene, which possess allylic hydrogen atoms are oxidized in the both positions, vinyl and allyl.

Our approach to finding an effective method for the gas phase epoxidation of propene was to use an oxygen-containing compound as an oxidant and a solid catalyst which can adsorb and activate it in such a manner that only mild electrophilic species will be generated.

Nitrous oxide has certain properties which make it suitable as a selective oxidant for the epoxidation of propene. Energetically, the release of an oxygen atom from  $N_2O$  is more favorable than from the oxygen molecule:



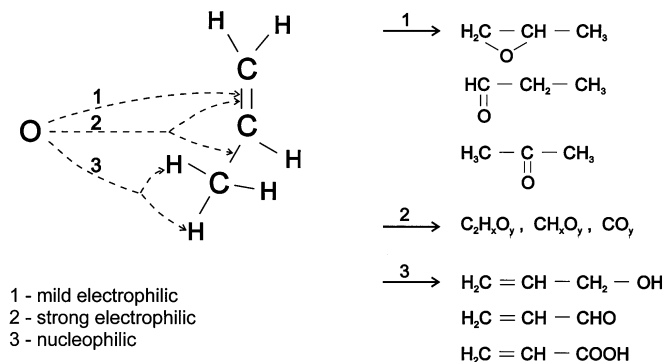
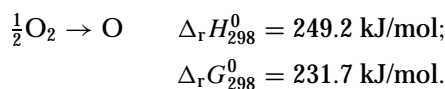
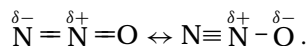


FIG. 1. Possible reaction paths of the reaction between propene and oxygen species.



The distribution of electrons in the  $N_2O$  molecule can be described by two mesomeric forms in resonance with each other (1c):



This distribution makes possible the adsorption of the  $N_2O$  molecule at cationic sites (6) and, consequently, the oxygen atom will obtain electrophilic properties (Fig. 2).

Several authors have already used  $N_2O$  as a selective oxidant but not for propene oxidation. Ohtani *et al.* (7) partially oxidized various organic substrates viz. alcohols, ethers, and amines in an aqueous suspension of platinum particles. Other authors (8–12) used  $N_2O$  for the partial oxidation of benzene to phenol. They chiefly used metal-doped zeolites as catalysts. Such catalysts cannot be used in the epoxidation of propene for two reasons: the high acidity of the catalysts and the strong activities in the decomposition of  $N_2O$  with the formation of very reactive oxygen species.

The catalyst for the epoxidation of propene must adsorb and activate the  $N_2O$  molecule without decomposing it. Furthermore, the catalyst must not have strong acidic and basic properties because under such conditions propene oxide can easily isomerize to propanal and acetone (1a, 2, 5) as already mentioned. Thus, silica gel was chosen as the catalyst support, which offers a high surface area, low acidity, and no intrinsic activity in  $N_2O$  decomposition. In order

to improve the adsorption capacity of silica the use of a highly dispersed transition metal oxide as an active component should be effective. In a comparison (13) between the activity of oxides of several 3d transition metals in the  $N_2O$  decomposition, it is shown that  $Fe^{3+}$  and  $Fe^{2+}$  ions have the lowest level of activity. In another investigation (14) of the  $N_2O$  decomposition activities of several catalysts, supported iron oxide shows again one of the lowest rates of activity. Drago *et al.* (15) found as well a very low activity level of silica-supported iron oxide in the decomposition of  $N_2O$ . Furthermore, alkali promotion and high temperature calcination are suitable measures for reducing the acidity of the catalyst. For these reasons, catalysts were prepared in the present study by doping various silica gels with small amounts of iron oxide, followed by sodium impregnation and calcination (16, 17).

## EXPERIMENTAL

### Materials

#### A. Catalyst Preparation

*Group a.* The silica gel support for this group of catalysts was prepared after (18) from tetraethylorthosilicate (TEOS), ethanol, *i*-propanol, 1-dodecylamine, and water. After calcination in air at 873 K, portions of this silica gel support (further named D) were impregnated by incipient wetness method with solutions of different concentrations of Fe(III)-acetylacetonate in toluene. The so-prepared catalysts were dried and then calcined at 873 K in air. To decrease the acidity of the catalysts (neutralization procedure), they were impregnated for 48 h in an aqueous solution of sodium acetate (Naac) and, after filtration and washing with distilled water, calcined at a temperature of 973 K for 6 h in air.

*Group b.* The support used for this group of catalysts was a silica gel from Degussa (Aeroperl 380/50, hereafter referred to as A), produced from  $SiCl_4$  by the flame hydrolysis process. The catalysts were prepared by the same procedure as the group a catalysts.

*Group c.* For this group of catalysts a silica gel with an iron content of 6 ppm from Merck (M60 reinst, hereafter referred to as Mr) was used as support. The catalysts were prepared by the same procedure described for the group a catalysts.

The iron loadings of the catalysts were 100, 300, 1000, and 10,000 ppm. The concentrations of the aqueous solutions of Naac used in the neutralization procedure were 0.01 M Naac (abbreviated N1), 0.1 M Naac (N2), and 1 M Naac (N3).

*Nomenclature of the catalysts.* The name of the catalysts was formed from a symbol for the support (D for the group a, A for group b, and Mr for group c), followed by the

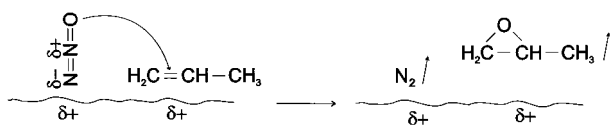


FIG. 2. Reaction step between propene and nitrous oxide toward propene oxide.

chemical symbol for iron, and a number which indicates the iron content of the catalyst in ppm, followed by the abbreviation which indicates the concentration of the aqueous sodium acetate solution used in the neutralization procedure. For example, AFe300N2 is the name for a catalyst with a support consisting of Aeroperl 380/50. The iron content is 300 ppm and the concentration of the neutralizing solution was 0.1 M Naac.

### B. Reactant Gases

The reactant gases used were propene of 99.5 vol% minimum purity, N<sub>2</sub>O of 99.5 vol% minimum purity, and helium of 99.996 vol% minimum purity, all of them from Messer Griesheim.

### Catalyst Characterization

The catalysts were characterized by means of nitrogen physisorption, powder X-ray diffraction (XRD), temperature-programmed reduction and oxidation (TPR-TPO), and temperature-programmed desorption (TPD).

*Determination of textural properties.* The specific surface areas and the porosities of the supports and catalysts were established by nitrogen physisorption at liquid nitrogen temperature (77 K) according to the BET method. The adsorption-desorption isotherms were recorded with a Sorptomatic 1990 apparatus (Fisons Instruments), equipped with a Milestone 200 software. A surface area requirement of 0.162 nm<sup>2</sup> for the physically adsorbed N<sub>2</sub> molecule was used for the calculation of the BET surface area. The pore size distribution was calculated with the Dollimore-Heal method. The samples were outgassed at 130°C for 2 h and then at room temperature overnight prior to the measurements; the residual pressure was about 10<sup>-6</sup> mbar.

*Powder X-ray diffraction.* Powder XRD was carried out in a HZG4 diffractometer from Seifert-FPM using a generator at 40 kV and 35 mA, a Ni filter, and CuK $\alpha$  radiation ( $\lambda = 1.540598 \text{ \AA}$ ).

*Temperature-programmed reduction and oxidation (TPR-TPO).* The apparatus consisted of a gas supplying unit, a quartz-tube reactor (6 mm i.d.) and a thermal conductivity detector. The reactor with a catalyst sample (ca. 0.3 g) was placed into an electrically heated oven. A gas stream of 30 ml/min with 10% H<sub>2</sub> in N<sub>2</sub> (for TPR) or of 40 ml/min with 12.5% O<sub>2</sub> in He (for TPO) was passed through the catalyst sample. The temperature of the sample was controlled via a thermocouple and was raised from room temperature at 30 K/min to 973 K and then held constant at this temperature for 30 min. The water produced by the reduction was condensed in a CO<sub>2(g)</sub>/*i*-propanol cooled trap. The amount of H<sub>2</sub>/O<sub>2</sub> consumption was detected via the thermal conductivity cell.

*Temperature-programmed desorption (TPD).* The TPD was carried out on catalyst samples (ca. 0.3 g) which were filled in a TPD cell made of quartz. The TPD cell was placed into an electrically heated oven and was connected to a main system which permitted either the outgassing of the cell or the gas supplying. The catalyst sample in the TPD cell was outgassed at a pressure of less than 10<sup>-6</sup> mbar for 30 min at room temperature. The TPD cell was then heated to 973 K and evacuated at this temperature for 60 min. The temperature of the cell was then adjusted to the adsorption temperature and the adsorbate gas was permitted to enter the TPD cell. After 30 min, the TPD cell was cooled down to room temperature and evacuated up to 10<sup>-2</sup> mbar. The TPD cell was then connected to a quadrupole mass spectrometer (QTMD-System from Fisons Instruments) and evacuated up to a pressure of less than 10<sup>-6</sup> mbar for 2 h. The TPD cell was heated up to 973 K with a heating rate of 5 K/min and then held at this temperature for 20 min. Six different molar masses (M) were continuously monitored in the course of desorption.

### Oxidation Experiments and Product Analysis

The propene oxidation experiments were carried out in a fixed-bed quartz-tube reactor (10 mm i.d.) under an absolute pressure of 1200 mbar using a continuous-flow system. The reactor, placed vertically, was surrounded by an electrical heater. The reactor temperature was measured and controlled via a thermocouple placed within the catalyst bed. The gaseous reactants were fed using mass flow controllers from Brooks. The reaction products were analyzed on-line using an IR-photometer from Rosemount to detect CO<sub>2</sub> and a gas chromatograph 5890 II Plus from Hewlett-Packard for the other products. The gas chromatograph was equipped with two capillary columns viz. Molsieb 5A and FFAP connected with a TCD and a FID, respectively, which enabled the analysis of O<sub>2</sub>, N<sub>2</sub>, CO, and N<sub>2</sub>O by the former and organic products by the latter detector.

The catalyst (usually 1 g) was placed into the reactor, near the bottom, on a porous quartz frit. Before each propene oxidation experiment, the catalyst was oxidized at 793 K in an air flow in order to remove remaining organic compounds from the previous experiment and to yield a high oxidation state of the active component. When no more CO<sub>2</sub> was detected in the outgas, the reactor temperature was adjusted to the desired oxidation temperature for the reaction experiment. Then, the air flow was replaced by a flow mixture of N<sub>2</sub>O (the needed flow value for the reaction) and He (the rest to balance the needed total flow). When the N<sub>2</sub>O concentration at the outlet of the reactor was constant, propene was added to the flow mixture and the flow of He was correspondingly diminished to keep the total flow constant. This moment was considered as the initial time point (time-on-stream = 0) for the oxidation experiment.

TABLE 1  
Textural Parameters of Selected Supports and Catalysts

Parameter	Support catalyst:		Group a		Group b		Group c	
	D	DFe300N2	A	AFe300N2	Mr	MrFe300N2		
Specific surface area (m <sup>2</sup> /g)	1167	511	314	229	420	332		
Specific pore volume (cm <sup>3</sup> /g)	1.84	0.74	1.28	1.38	0.83	0.63		
Relative volume (%) for pore ranges								
100–10 nm	<b>55.1</b>	<b>64.4</b>	<b>79.3</b>	<b>86.8</b>	0.7	0.3		
10–5 nm	1.8	7.3	6.4	10.1	4.4	4.2		
5–2 nm	4.2	6.9	6.7	2.7	<b>87.7</b>	<b>89.7</b>		
2–1.5 nm	8.7	5.2	0.8	0.0	5.3	4.2		
1.5–1 nm	<b>30.0</b>	<b>16.0</b>	2.0	0.0	1.7	1.3		
<1 nm	0.0	0.0	0.0	0.1	0.0	0.0		

During the oxidation experiments the reaction parameters (pressure, temperature, gas flow composition, and velocity) were kept constant and the reaction products were continuously analyzed by the IR-photometer and periodically by the gas chromatograph. After a period of time the experiment was stopped; the flows of propene, nitrous oxide, and helium were interrupted and the catalyst was regenerated by oxidation at 793 K in a flow of air.

## RESULTS

### Catalyst Characterization

The determined textural parameters of selected supports and catalysts are summarized in Table 1. The support D had a very high specific surface area and a large specific

pore volume, but after the iron and sodium impregnation and calcination the same parameters of the corresponding catalyst (DFe300N2) had less than 50% compared to the initial values. Especially the narrow pores of the catalyst suffered a severe shrinking. The catalysts prepared with the supports A and Mr show surface area losses of less than 30% compared to the related supports. They preserved their specific pore structure with larger pores in the case of A and with a narrow distribution in the range of slim mesopores in the case of Mr.

The XRD spectra for support A, some selected catalysts, and a sample of iron oxide prepared from the same iron precursor, using the same procedure as with the catalysts, are shown in Fig. 3. The XRD spectra of the support and catalysts showed no crystalline features for silicium oxide or for iron oxide. In contrast, the iron oxide sample showed

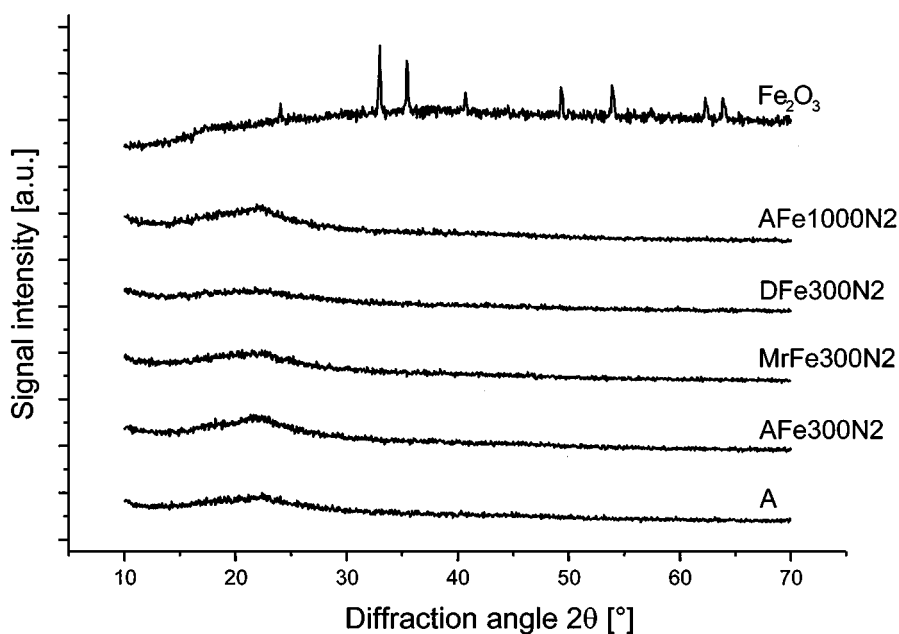


FIG. 3. XRD spectra of support A, selected catalysts, and an Fe<sub>2</sub>O<sub>3</sub> sample.

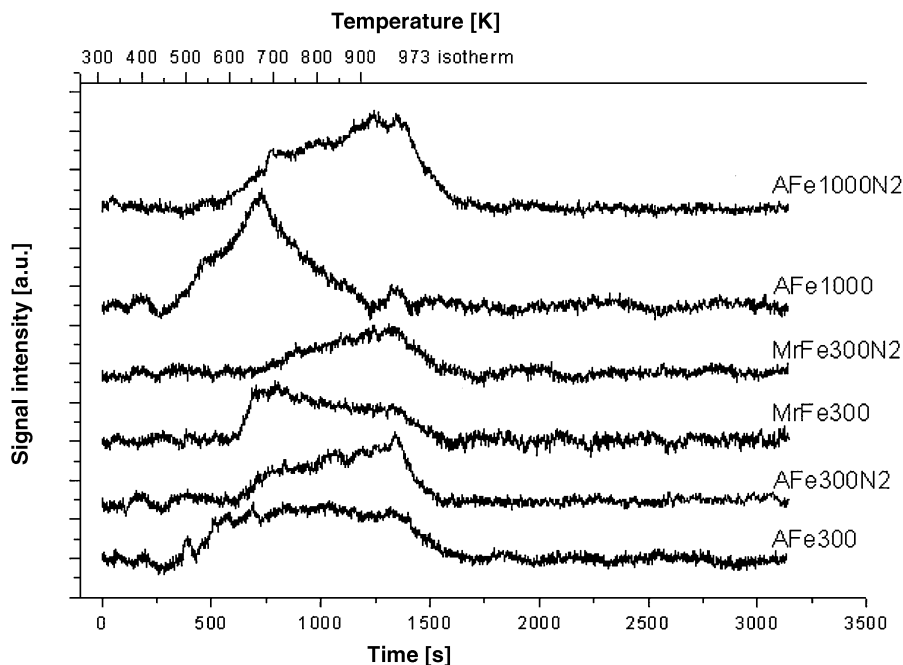


FIG. 4. TPR spectra of Na-promoted and unpromoted silica supported  $\text{Fe}_2\text{O}_3$  catalysts.

the characteristic peaks of different  $\text{Fe}_2\text{O}_3$  crystalline phases.

The TPR spectra for catalysts with 300 and 1000 ppm Fe content as well as with and without sodium are shown in Fig. 4. Despite the weak intensity of the signals due to the small amounts of iron oxide, one can see a shifting of the

reduction temperatures toward higher values for the Na-impregnated catalysts than for the corresponding catalysts which were not Na-impregnated.

The desorption spectra of propene using catalyst AFe300N2 is depicted in Fig. 5. It shows three desorption regions with signals at about 350, 730, and 950 K in which

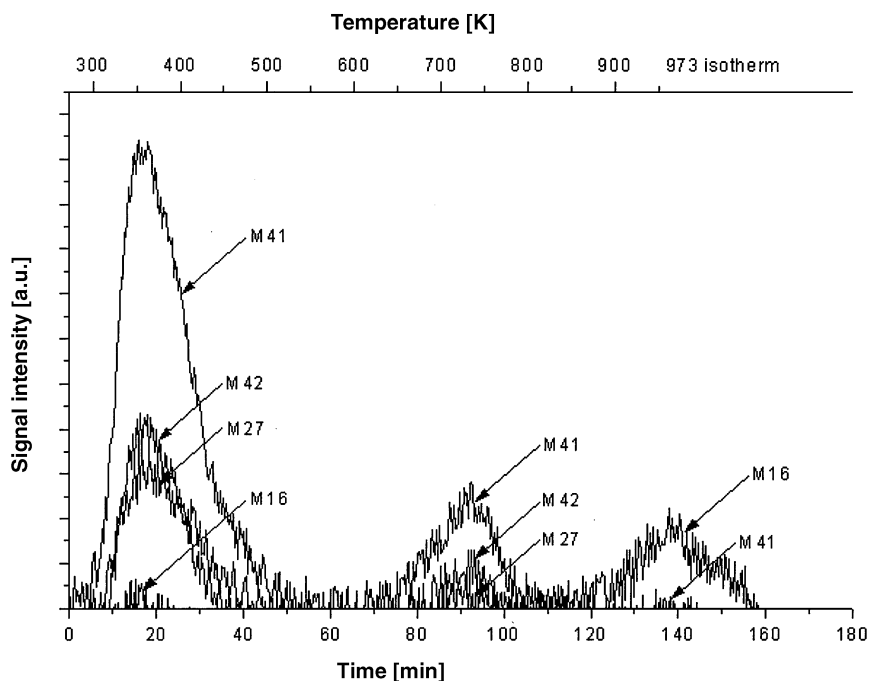
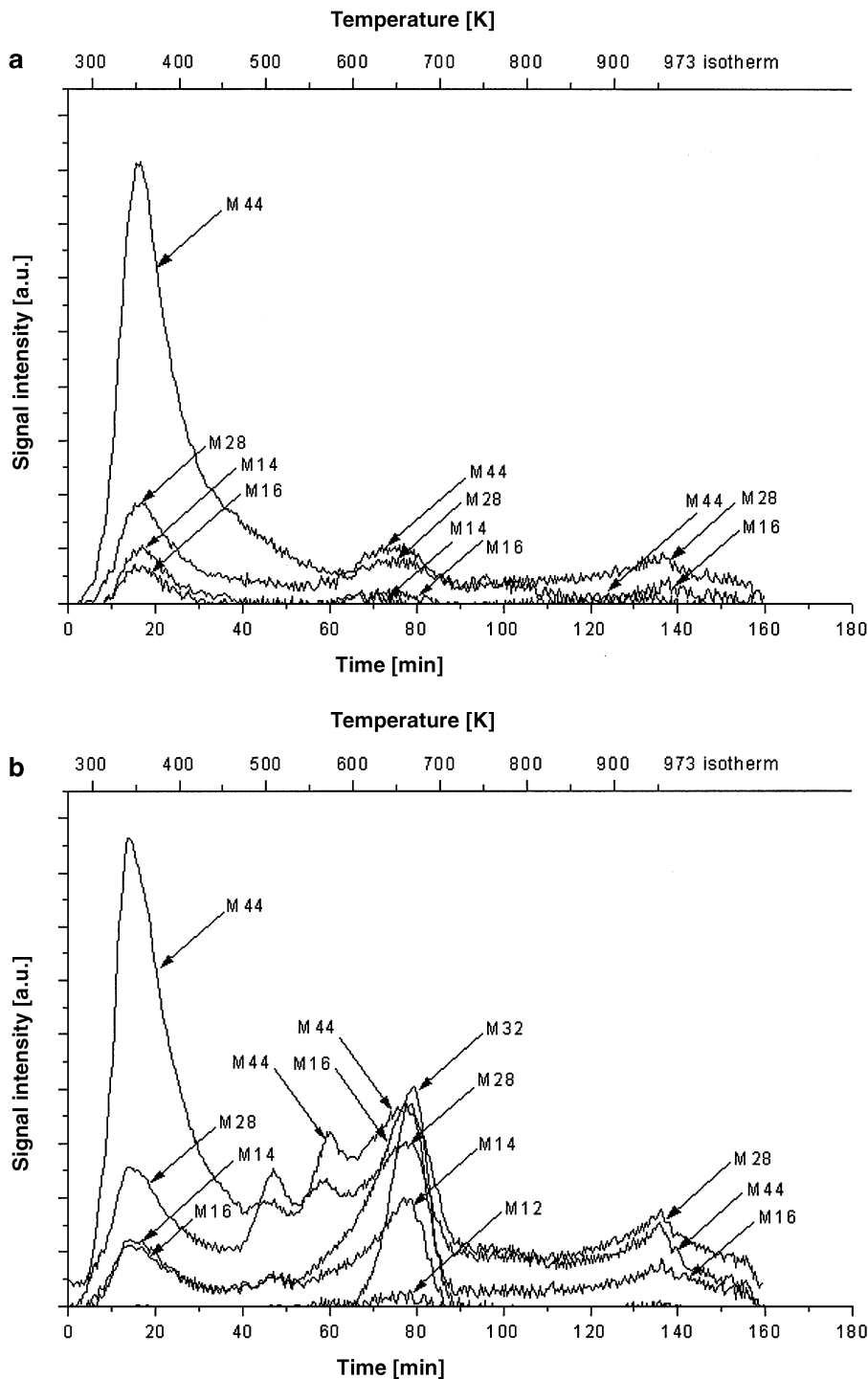


FIG. 5. TPD spectra of propene desorbed from the catalyst AFe300N2.



**FIG. 6.** TPD spectra of nitrous oxide by the desorption from the catalysts (a) AFe300N2, (b) AFe10000N2, (c) MrFe300N2, and (d) AFe300N2, DFe300N2, and MrFe300N2 (only the M44 signal).

various decomposition fragments of propene appear. Six molar masses of 12, 15, 16, 27, 41, and 42 were monitored. The first desorption region for propene can be assigned to the desorption of physically adsorbed propene and the second and third region to that of chemisorbed species.

The desorption spectra of nitrous oxide (Fig. 6) from the catalysts AFe300N2 (Fig. 6a), AFe10000N2 (Fig. 6b), and MrFe300N2 (Fig. 6c) show the six monitored molar masses of 12, 14, 16, 28, 32, and 44 and mirrors two important features. On one hand, the  $N_2O$  signal (molar mass 44,

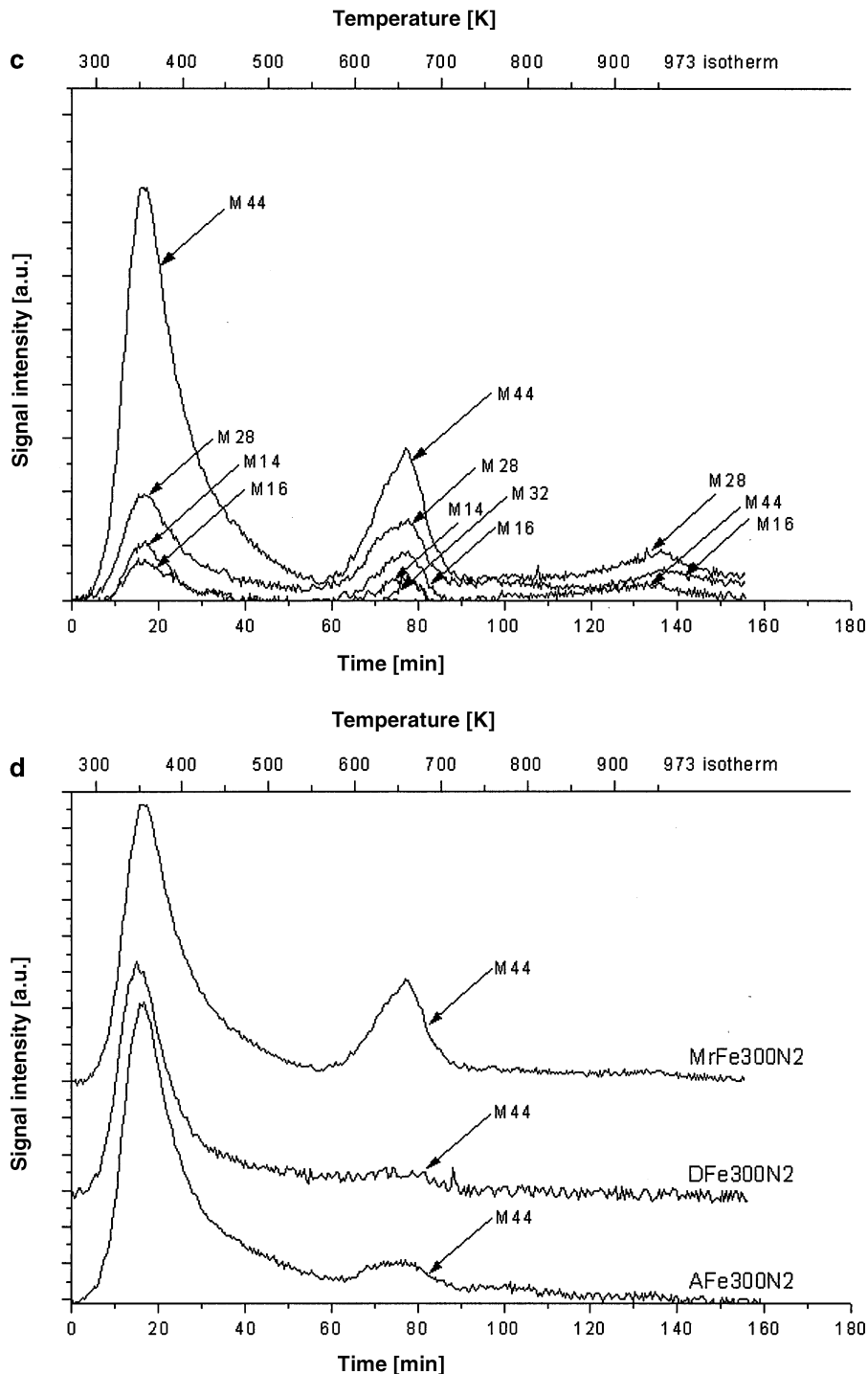


FIG. 6—Continued

M44) was always accompanied by signals stemming from nitrogen (M14) and oxygen (M16), which can emerge from  $N_2O$  decomposition in the vacuum chamber of the mass spectrometer. As far as these signals always accompanied the  $N_2O$  desorption signal, they were not used to interpret the nature of the  $N_2O$  adsorption. On the other hand, the appearance of  $O_2$  (M32), which necessitates the decom-

sition of  $N_2O$  and the recombination of two oxygen atoms, and which did not necessarily accompany the  $N_2O$  signal, was used as an indication for a dissociative adsorption of  $N_2O$  in the respective case.

Three distinct groups of desorption peaks appear, one of them slightly over room temperature (ca. 350 K) and the other two at high temperatures of about 650 and 950 K.

The low-temperature group of desorption peaks can be assigned to a physically adsorbed  $N_2O$  form, while the high-temperature groups of desorption peaks were assigned to a chemically adsorbed  $N_2O$  form. In the TPD of  $N_2O$  from the supports A, D, and Mr (not shown) only the low temperature desorption peaks at ca. 350 K appeared. The catalyst with an iron loading of 1% (AFe1000N2) showed a strong desorption peak of molecular oxygen (M32) at about 650 K (Fig. 6b). The two depicted desorption spectra for catalysts with 300 ppm Fe (AFe300N2 and MrFe300N2) showed no or very weak desorption peaks of molecular oxygen (Figs. 6a and 6c). The catalysts with 1000 ppm Fe (not shown) presented weak M32 desorption signal intensity. The comparison between the desorption spectra for M44 from three catalysts with an iron content of 300 ppm (Fig. 6d) showed similar intensities at ca. 350 K but different ones at ca. 650 K. That means that the physisorption ability of these catalysts is similar but the chemisorption ability increases in the order  $DFe300N2 < AFe300N2 < MrFe300N2$ .

In addition, CO adsorption measurements were carried out over prerduced (in a flow of  $H_2$ ) catalyst samples in order to determine the exposed surface and dispersy of iron, but because of the very small amounts of iron it was not possible to carry out quantitative determinations.

### Oxidation Experiments

In order to investigate the influence of the  $N_2O$  concentration on the catalytic results, a series of catalytic runs were carried out at a constant propene concentration of 1% and different  $N_2O$  concentrations. The effect of the  $N_2O$  concentration and the time on stream (TOS) on the reaction rate and selectivity for the catalyst DFe300N2 can be seen in Fig. 7. For the set propene concentration, the reaction rate increased with increasing  $N_2O$  concentration up to a con-

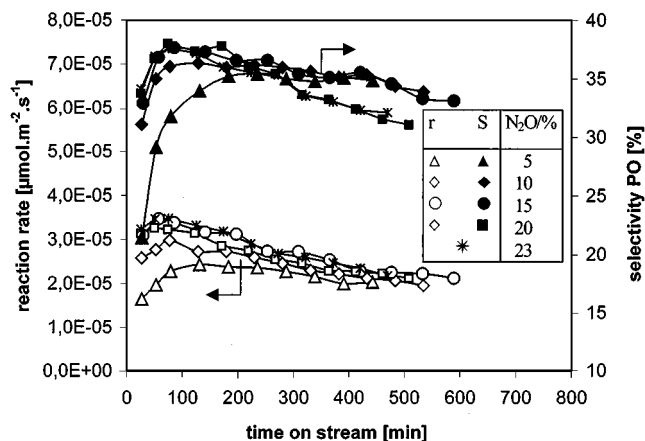


FIG. 7. Reaction rate of propene and selectivity to propene oxide at different  $N_2O$  concentrations. Reaction parameters: 1% propene,  $N_2O$  variable, balance He; catalyst DFe300N2; reaction temperature 648 K; GHSV =  $4 L h^{-1} g^{-1}$  (STP).

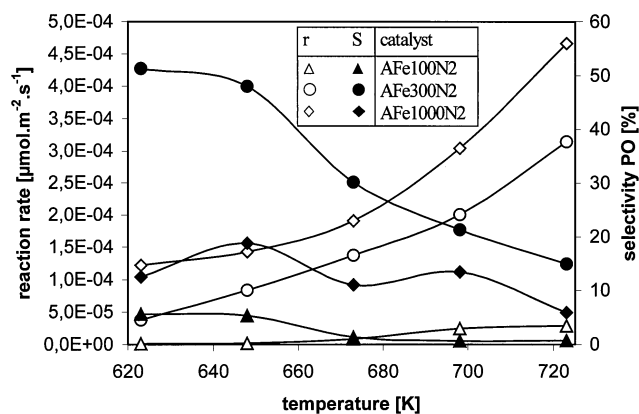


FIG. 8. Reaction rate of propene and selectivity to propene oxide over catalysts with different iron loadings. Reaction parameters: 1% propene, 15%  $N_2O$ , 84% He; GHSV =  $4 L h^{-1} g^{-1}$  (STP); TOS = 77 min.

centration of 15%  $N_2O$  and then remained approximately constant. After reaching maximum values, the reaction rate had a slight decrease with the time on stream. The selectivity toward propene oxide also increased with the  $N_2O$  concentration up to a concentration of 15% and increased in the first 100 min of TOS for all  $N_2O$  concentrations. For  $N_2O$  concentrations of 10% or more the selectivity reached a maximum after 100–200 min TOS and then began to decrease. The higher the  $N_2O$  concentration, the higher the yield. As a consequence of these evolutions, the yield to propene oxide generally reached the maximum at a concentration of 15%  $N_2O$ . Similar results were obtained for the other catalysts as well.

The influence of the iron content of the catalysts on the catalytic performance is exemplified in Fig. 8 for a series of catalysts. All of them have the same support (A, i.e., Aeroperl 380/50) with large pores which do not restrict the iron oxide particles grown during the preparation procedure and were Na-promoted after the same procedure. The results were recorded after a time on stream of about 77 min. The reaction rate increased in the entire investigated temperature range with the iron loading and the selectivity reached a maximum at an iron loading of 300 ppm. Catalysts with an iron loading of 1% (10000 ppm; not shown) had a higher activity than the ones with 1000 ppm but the selectivity to propene oxide was very low.

As already mentioned, in order to neutralize the acidity of the catalysts, they were impregnated with a Na-solution and after that they were calcinated. In Fig. 9 a comparison is shown between the activities (Fig. 9a) and selectivities to propene oxide (Fig. 9b) for a series of catalysts with an iron loading of 300 ppm but which have undergone different Na-impregnation treatments. The oxidation activity expressed as propene reaction rate generally increased with the sodium loading (Fig. 9a). The selectivity to propene oxide was very low over the non-sodium-impregnated catalyst, increased with the Na loading, reached a maximum for the impregnation in the intermediate

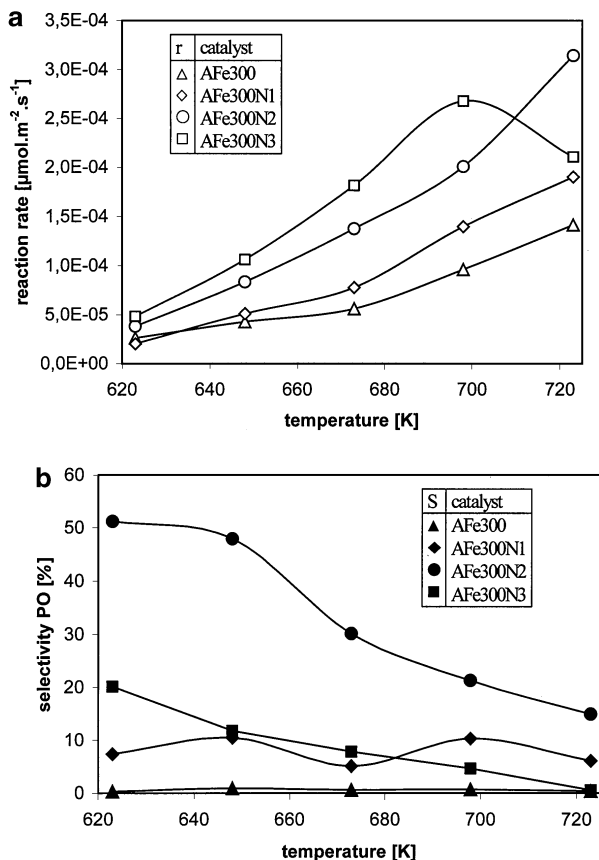


FIG. 9. Reaction rate of propene (a) and selectivity to propene oxide (b) over catalysts with different Na-impregnation treatments. Reaction parameters: 1% propene, 15%  $N_2O$ , 84% He; GHSV =  $4 \text{ L h}^{-1} \text{ g}^{-1}$  (STP); TOS = 77 min.

concentration of 0.1 mol/L aqueous solution of sodium acetate, and decreased with further increase of the Na loading (Fig. 9b).

In Fig. 10 a comparison is made between three catalysts with the same iron content and which have undergone the same neutralization treatment but with different supports. The catalyst with slim mesopores (MrFe300N2) shows a higher reaction rate and selectivity than the other two catalysts (Fig. 10a). Consequently, the yield to propene oxide over MrFe300N2 was considerably higher than over the other two catalysts and reached values of ca. 5% (Fig. 10b). In addition, data of conversions and selectivities to several identified products at different temperatures over the catalyst MrFe300N2 are given in Table 2.

The variation of the reaction rate and selectivity to propene oxide with time on stream at different gas hourly space velocities (GHSV) is represented in Fig. 11. The increase of the GHSV from 2 to  $4 \text{ L h}^{-1} \text{ g}^{-1}$  brought a significant increase in the reaction rate and selectivity to propene oxide. A further increase of GHSV to  $6 \text{ L h}^{-1} \text{ g}^{-1}$  brought no alteration of the reaction rate; however, the selectivity was somewhat higher at the beginning of the experiment but decreased faster with increasing TOS.

TABLE 2  
Conversions and Selectivities over MrFe300N2

Temperature (K)	573	598	623	648	673	698	723
Conversion propene (%)	0.6	2.5	6.1	10.1	11.9	20.3	29.0
Selectivities (%)							
Propene oxide	62.3	70.0	60.1	48.1	39.7	23.9	12.2
Propanal	9.1	7.0	6.8	6.6	7.1	5.0	3.4
Acetone	5.3	5.7	7.8	9.6	11.0	8.2	8.2
Allyl alcohol	10.9	6.1	5.1	5.2	5.8	7.9	5.6
Acrolein	8.8	2.9	3.2	3.8	4.5	5.2	3.9
Carbon monoxide	0.0	2.9	6.9	10.7	14.8	26.3	39.0
Carbon dioxide	0.0	2.5	4.3	9.5	8.9	15.5	19.5

Note. Reaction parameters: 1% propene, 15%  $N_2O$ , 84% He; GHSV =  $4 \text{ L h}^{-1} \text{ g}^{-1}$  (STP); TOS = 128 min.

In order to find out the regeneration capability of the catalyst, two reaction experiments were carried out with the same catalyst under identical conditions (Fig. 12). After the first oxidation run was carried out, seven reaction-regeneration cycles were performed at different temperatures. The ninth reaction experiment was then carried out

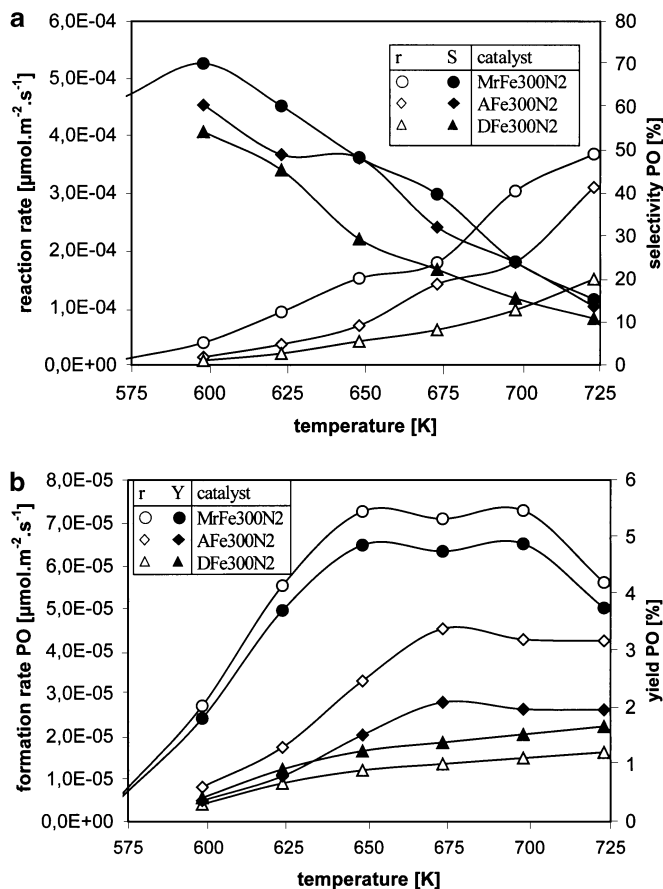


FIG. 10. Reaction rate of propene and selectivity to propene oxide (a) and formation rate of and yield to propene oxide (b) over catalysts with different supports. Reaction parameters: 1% propene, 15%  $N_2O$ , 84% He; GHSV =  $4 \text{ L h}^{-1} \text{ g}^{-1}$  (STP); TOS = 128 min.

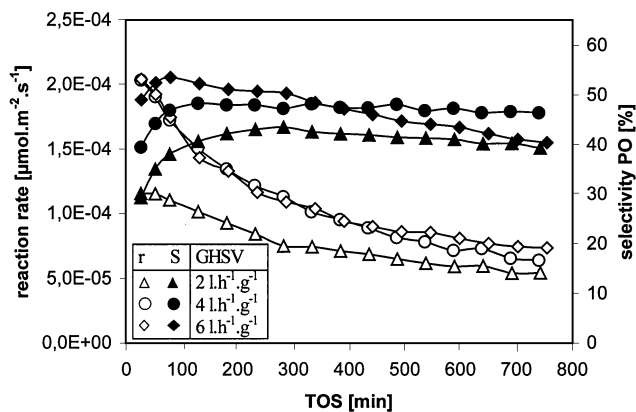


FIG. 11. Reaction rate of propene and selectivity to propene oxide as a function of TOS at different gas hourly space velocities. Reaction parameters: 1% propene, 15% N<sub>2</sub>O, 84% He; catalyst MrFe300N2; reaction temperature 648 K.

at the conditions of the first run. The results are depicted in Fig. 12 and show that the reaction rate and the selectivity to propene oxide had similar values in both runs.

The yields and selectivities to several products vs TOS are given in Fig. 13. The yields to propene oxide, to its isomers propanal and acetone, and to the carbon oxides have a similar descendent course. On the other hand, the yield to allyl oxidation products like allyl alcohol and acrolein has a different course and remains approximately constant. From Fig. 13 the selectivity-conversion behavior was derived and depicted in Fig. 14. In spite of the deactivation during the oxidation experiment indicated by the conversion decrease, the selectivity to propene oxide of ca. 48% was nearly constant in the range of 5–10% conversion degree.

## DISCUSSION

First investigations into the possibility of producing propene oxide by the gas phase reaction between propene and

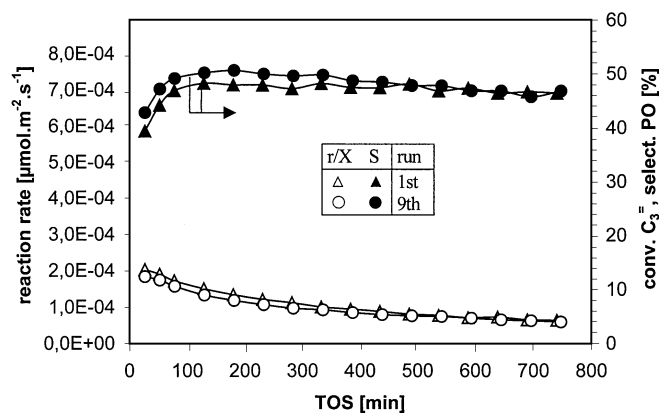


FIG. 12. Reaction rate of propene and conversion and selectivity to propene oxide for two oxidation runs at identical conditions. Reaction parameters: 1% propene, 15% N<sub>2</sub>O, 84% He; catalyst MrFe300N2; reaction temperature 648 K; GHSV = 4 L h<sup>-1</sup> g<sup>-1</sup> (STP).

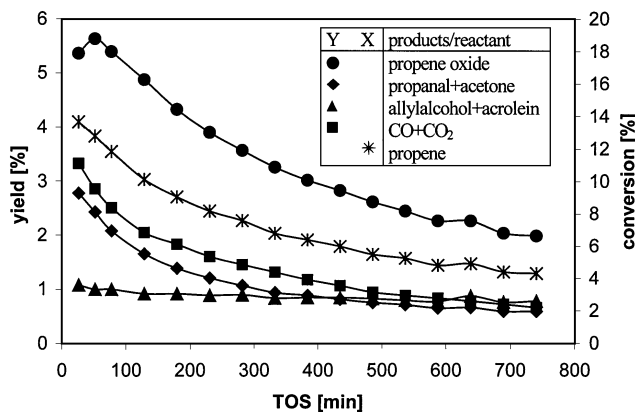


FIG. 13. Conversion of propene and yields to products vs TOS. Reaction parameters: 1% propene, 15% N<sub>2</sub>O, 84% He; catalyst MrFe300N2; reaction temperature 648 K; GHSV = 4 L h<sup>-1</sup> g<sup>-1</sup> (STP).

nitrous oxide over iron-oxide-containing catalysts were successful (16) and have led to the current in-depth investigation of the factors which influence the catalytic performance in this reaction (17).

The preparation of the catalysts was focused on obtaining catalysts with different iron loadings, neutralization procedures, and porosities. The reaction parameters were varied to study the effect of reactant composition, reaction temperature, gas hourly space velocity, and time on stream on activity and propene oxide selectivity. Furthermore, the possibility of regenerating the catalysts after a reaction experiment and the products distribution was also studied.

The experiments with catalysts having different iron loadings illustrated that the catalytic results depend strongly on the iron loading of the catalysts (Fig. 8). The increase of the reaction rate is not directly proportional to the iron loading. This means that it is not the iron oxide amount that directly determines the activity of the catalysts. The evolution of the reaction rate and selectivity to

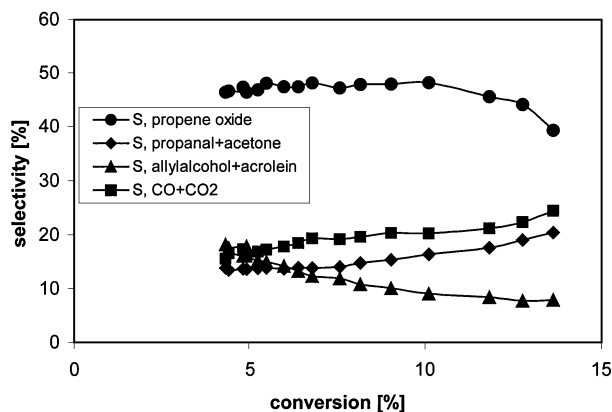


FIG. 14. Selectivities to products vs conversion. Reaction parameters: 1% propene, 15% N<sub>2</sub>O, 84% He; catalyst MrFe300N2; reaction temperature 648 K; GHSV = 4 L h<sup>-1</sup> g<sup>-1</sup> (STP).

propene oxide with the iron loading suggests that the iron oxide particle dimension plays an important role in the catalytic activity. In other words, very small iron oxide particles in the catalysts result in a low activity and selectivity toward propene oxide, somewhat larger iron oxide particles (corresponding to an iron loading of ca. 300 ppm) have a much higher activity and selectivity, and with a further increase of particle dimension the activity continues to increase slowly, but the selectivity to propene oxide goes down. According to the XRD investigations, the iron oxide particles in all used catalysts have diameters less than 2 nm (13b). Attempts to determine more exactly the particle dimension and the dispersity of the iron oxide by adsorption measurements failed because of the experimental difficulties bounded with the very small amounts of iron oxide that are present in the catalysts.

The Na impregnation of the catalysts generally had a positive impact on activity. Less severe or no Na impregnation led to a fast deactivation of the catalysts, so the activity was considerably lower after the same time on stream (Fig. 9a). A more severe Na impregnation (as for the catalyst AFe300N3) led to a lower activity at high temperatures. This means that an excess of Na can also lead to a faster deactivation of the catalysts. The evolution of the selectivity with the Na-impregnation treatment showed that there is an optimal impregnation treatment leading to a maximum in selectivity.

The three silica gel supports used in the present investigation had distinct textural properties which make them suitable for studying the effect of support porosity on the morphologic and catalytic properties of this kind of catalysts (Table 1). The support D had an important proportion of narrow pores. This was considerably diminished after the catalyst preparation, where the first step was the impregnation of the support with the iron precursor. That leads to the assumption for the group a catalysts that an important part of the iron oxide particles is located inside the narrow pores. As a consequence, the localization of the active centers in narrow pores can improve the adsorption capacity of the catalyst but can also lead to the appearance of diffusion problems. The catalysts from group b have large pores, which permit a sufficient diffusion of the reactants and products; however, this kind of pore cannot contribute a great deal to the adsorption process. The catalysts from group c combine the presumptive advantages of the catalysts from groups a and b, creating a better contribution of their slim mesopores to the adsorption process than the larger pores of the catalysts of group b and less severe diffusion problems than the catalysts of group a. A schematic representation of the catalyst pore structures is shown in Fig. 15. The described properties can be discussed also with respect to the porosity of the catalysts which strongly influenced the performance of the catalysts, as seen in Fig. 10. The catalyst with a considerable proportion of narrow pores (DFe300N2) showed the lowest activity and selectivity. This

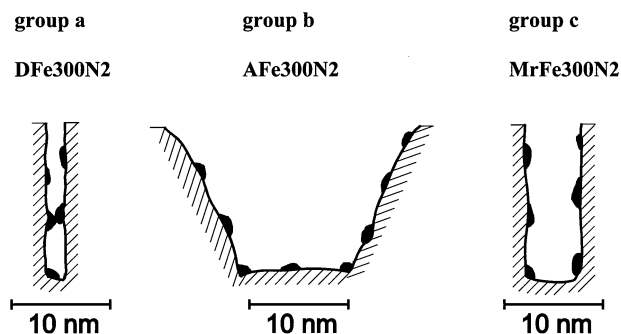


FIG. 15. Schematic representation of the catalyst pore structure with iron oxide particles smaller than 2 nm.

means that the narrow pores have a negative influence on the oxidation of propene to propene oxide, probably due to the appearance of desorption and/or diffusion difficulties. The catalyst with large pores (AFe300N2) showed better results than DFe300N2, but the catalyst with almost exclusively slim mesopores (MrFe300N2) had the best performance. Such pores can contribute to the adsorption process of the reactants without considerably hindering the desorption and diffusion of products.

For a set propene concentration, the reaction rate of propene increased with the concentration of the oxidant ( $N_2O$ ). The selectivity to propene oxide initially increased with the  $N_2O$  concentration but beyond a certain  $N_2O$  concentration, the selectivity to propene oxide decreased because of a stronger oxidation of propene to deeper oxygenated products.

Generally, the reaction rate increased and the selectivity to propene oxide decreased with increasing temperature (Figs. 8–10). The maximal yield to propene oxide was reached at approx. 650–700 K (Fig. 10b).

The experiments carried out at different space velocities led us to the conclusion that at values lower than  $4 \text{ L h}^{-1} \text{ g}^{-1}$  there are some external diffusion hindrances that limited the reaction rate of propene and selectivity to propene oxide (Fig. 11).

The results from the experiments depicted in Fig. 12 showed the good regeneration capability of the catalysts. After a few reaction–regeneration cycles, the activity becomes somewhat lower but the selectivity becomes a little higher, so the yield to propene oxide remains approximately constant for more than 50 reaction–regeneration cycles.

The similar course for the yields (i.e., the rates of formation) to vinyl oxidation products (propene oxide, propanal, acetone) and carbon oxides (Fig. 13) means that these products are formed over the same active centers and according to similar formation rate equations. The decrease of the rates of formation for these products can be associated with a deactivation of the active centers, which are responsible for the adsorption of  $N_2O$ . In contrast, the allyl oxidation products allyl alcohol and acrolein which are most probably produced by a Mars–van Krevelen mechanism over

the redox centers of the catalyst, are not affected by this deactivation.

The reaction rate of propene always decreased slightly with the TOS but the selectivity to propene oxide was approximately constant. After the regeneration of the catalyst by oxidation in air, the catalyst regained its initial activity. In the course of the air regeneration of the catalyst, carbon oxides were detected in the exhaust from the reactor. The carbon oxides can originate from carbonaceous deposits and/or strongly adsorbed hydrocarbon species. Two factors could contribute to the reversible decrease of the reaction rate with TOS. On one hand, the physical blocking of some adsorption centers by these deposits and strong adsorbed species can gradually lead to a decrease of the reaction rate with time. On the other hand, the chemical reduction of the active centers under the reaction conditions could also contribute to a decreasing number of active centers with time. The impregnation with sodium reduced the acidity and increased the reduction temperature of the catalysts (Fig. 4). As a result, the reaction rate was higher (Fig. 9a). An excess of basicity can have a reverse effect, as evidenced by the catalyst AFe300N2 at higher temperatures (Fig. 9a).

The selectivity to propene oxide increased with TOS at the beginning of an experiment. In this period of time (approx. 100–200 min) the most active centers, which lead to a deeper oxidation, are probably deactivated and this has positive effects on the selectivity (Figs. 7, 11, and 12). After this period, the selectivity to propene oxide went slowly down. The decrease of the propene oxide selectivity is more pronounced at higher temperatures, N<sub>2</sub>O concentrations, and space velocities. The decrease of the propene oxide selectivity can be explained by a further deactivation of the adsorption centers, in contrast to the redox centers which produce allyl oxidation products and which are less affected by a deactivation process if at all (Fig. 13).

TPD experiments for propene and nitrous oxide were carried out in order to investigate the nature of the adsorbed species and thereby to contribute to the elucidation of the reaction mechanism. The silica gel supports showed only a desorption of the physisorbed N<sub>2</sub>O form, while the iron-oxide-containing catalysts showed a desorption of both N<sub>2</sub>O forms, physisorbed and chemisorbed. The catalysts with an iron content up to 1000 ppm (0,1%) showed little or no O<sub>2</sub> desorption. The catalysts with 10000 ppm (1%) Fe showed a relatively strong O<sub>2</sub> desorption signal. This indicates that the iron-free silica gels have no chemisorption capacity for N<sub>2</sub>O. Furthermore, the presence of small amounts of iron oxide on the surface of the catalysts lead to the nondissociative adsorption of N<sub>2</sub>O, and the presence of larger amounts of iron oxide lead, in complement with the latter, to a dissociative adsorption of N<sub>2</sub>O. In correlation with the catalytic experimental results, one can say that the nondissociative adsorption of N<sub>2</sub>O is a necessary condition for the epoxidation of propene in this system.

## SUMMARY

The present study describes a novel method of forming propene oxide by the heterogeneously catalyzed gas phase oxidation of propene with nitrous oxide. The catalysts consisted of silica-supported, sodium-promoted iron oxide. The optimal iron loading of the catalysts was in the range of 100–1000 ppm and the iron oxide particle dimension was smaller than 2 nm. The reaction occurred by the nondissociative adsorption of N<sub>2</sub>O at the active centers of the catalysts followed by the reaction between N<sub>2</sub>O and propene. The impregnation of the catalysts with alkali (sodium) was of great importance in order to minimize the side reactions and thereby to improve the selectivity toward propene oxide.

## ACKNOWLEDGMENT

The authors express their gratitude to the Fonds der Chemischen Industrie for financial support of this work.

## REFERENCES

1. "Ullmann's Encyclopedia of Industrial Chemistry," 5th ed. VCH, Weinheim. (a) Kahllich, D., Wiechern, U., and Lindner, J., Vol. A22, p. 239 (1993); (b) Rebsdatt, S., and Mayer, D., Vol. A10, p. 117 (1987); (c) Thiemann, M., Scheibler, E., and Wiegand, K. W., Vol. A17, p. 332 (1991).
2. Trent, D. L., in "Kirk-Othmer Encyclopedia of Chemical Technology," 4th ed., Vol. 20, p. 271. Wiley, New York, 1996.
3. (a) Clark, H. J., Maj, J. J., Bowman, R. G., Bare, S. R., and Hartwell, G. E., WO Patent 00415, 1998; (b) Bowman, R. G., Maj, J. J., Clark, H. W., Hartwell, G. E., Womack, J. L., and Bare, S. R., WO Patent 00414, 1998; (c) Bowman, R. G., Womack, J. L., Maj, J. J., Clark, H. W., and Hartwell, G. E., WO Patent 00413, 1998.
4. Gaffney, A., Kahn, A., and Pitchai, R., WO Patent 30552, 1998.
5. Coxon, J. M., MacLagan, R. G. A. R., Rauk, A., Thorpe, A. J., and Whalen, D., *J. Am. Chem. Soc.* **119**, 4712 (1997).
6. Ramis, G., Busca, G., and Bregani, F., *Gazz. Chim. Ital.* **122**, 79 (1992).
7. Ohtani, B., Takamiya, S., Hirai, Y., Sudoh, M., Nishimoto, S., and Kagiya, T., *J. Chem. Soc. Perkin Trans. II* **2**, 175 (1992).
8. Iwamoto, M., Hirata, J., Matzukami, K., and Kagawa, S., *J. Phys. Chem.* **87**, 903 (1983).
9. Suzuki, E., Nakashiro, K., and Ono, Y., *Chem. Lett.* **6**, 953 (1988).
10. Panov, G. I., Uriarte, A. K., Rodkin, M. A., and Sobolev, V. I., *Catal. Today* **41**, 365 (1998).
11. Burch, R., and Howitt, C., *Appl. Catal. A* **106**, 167 (1993).
12. Häfele, M., Reitzmann, A., Roppelt, D., and Emig, G., *Appl. Catal. A* **150**, 153 (1997).
13. "Handbook of Heterogeneous Catalysis" (G. Ertl, H. Knözinger, and J. Weitkamp, Eds.). VCH, Weinheim. (a) Cimino, A., and Stone, F. S., Vol. 2, p. 845 (1997); (b) Bergeret, G., and Gallezot, P., Vol. 2, p. 439 (1997).
14. Yamashita, T., and Vannice, A., *J. Catal.* **161**, 254 (1996).
15. Drago, R. S., Jurczik, K., and Kob, N., *Appl. Catal. B* **13**, 69 (1997).
16. Hönicke, D., Duma, V., and Krysmann, W., DE Patent Appl. 198 54 615.7-43, 11/26/1998.
17. Duma, V., Ph.D. thesis, in preparation, Technical University Chemnitz, Germany.
18. Gontier, S., and Tuel, A., in "Studies in Surface Science and Catalysis" (L. Bonneviot and S. Kaliaguine, Eds.), Vol. 97, p. 157. Elsevier, Amsterdam, 1995.